Electro-Optic Modulator in Thin-Film Lithium Niobate Foundry Process

Alberto Della Torre, Homa Zarebidaki, Jacopo Leo, Arno Mettraux, Gregory Choong,
Mattia Orvietani, Yves Petremand, Ivan Prieto, Olivier Dubochet, Michel Despont,
Hamed Sattari

Swiss Center for Electronics and Microtechnology (CSEM), Neuchatel, Switzerland

Abstract. The Characterization of thin-film lithium niobate modulators with electro-optical bandwidth higher than 50 GHz is presented. The devices, operating in the telecom C-band, are manufactured in a standard foundry process following design rules. The 7.95 mm long modulator has a half-wave voltage of 3.2 V and an extinction ratio of 15.4 dB. We also show that modulators, with the same design but fabricated in different wafers, present very similar performances, corroborating the reliability of the process design kit (PDK) component and the manufacturing process.

Keywords: Thin-Film Lithium Niobate, Electro-Optic Modulator, Foundry Process, Process Design Kit.

1 Introduction

In the last decade, electro-optical (EO) modulation in photonics integrated circuits (PICs) has witnessed remarkable advancements, mainly driven by the increasing bandwidth demand of quickly evolving telecom applications. In this respect, among the different PIC platforms, thin-film lithium niobate on insulator (TFLN) technology excels, offering unique properties like wide transparency, minimal optical loss, and a high electro-optic coefficient, making it an excellent choice for low-power, high speed optical modulators [1].

Different approaches have been adopted for optical modulation in various PIC platforms. In silicon, for instance, due to the lack of second-order nonlinearity, optical modulation schemes based on plasma dispersion have been proposed [2]. However, the trade-off between voltage, bandwidth, and optical losses poses fundamental limitations to the overall performances achievable by electronic doping. Thermo-optical [3] and micro-electro-mechanic systems (MEMS) [4] modulators have also been widely explored, but the slow thermal response of most materials and the mechanical movement of microstructures make them inherently slower than their EO counterpart. Plasmonics-based approaches, while fast and compact, suffer from high losses and need further tech development to achieve high scalability [5]. On the contrary, the superior EO of TFLN offer the opportunity to simultaneously achieve low-voltage and high-speed modulation [6]. In particular, voltage-length product of 1.2 V.cm [7] and bandwidth beyond 100 GHz [8] have been achieved in TFLN modulators. Yet, as compared to more mature PIC platforms like silicon and InP, TFLN manufacturing technology still needs further development to meet PIC industry's demands. The development of an open-access, standardized TFLN PIC platform is a crucial step towards the widespread use of this technology.

Here, we present the performance metrics of TFLN Mach-Zender EO modulators (MZM) manufactured in our standard foundry process. We also investigate the reliability of the manufacturing process by measuring devices from different wafers, and we show that the devices present similar performances.

2 Design and Fabrication

The layout of our standard MZI modulator demonstrating the technology layers is presented in Fig. 1(a). The circuit encompasses a series of optimized building blocks from the process design kit (PDK) library, such as MMI beam splitters, waveguide crossing, and edge couplers [9, 10]. We adopted a push-pull configuration for the electrodes with a pair of ground-signal-ground pads to minimize the half-wave voltage and facilitate the high-speed probing. For designing the MZM, simulations have been conducted to achieve a 50-ohm match condition for the modulator, considering the specific dimensions of the layers provided by the platform criteria. A signal electrode width of 13.7 µm and a signal gap of 4.5 µm were chosen to balance optical and RF losses while also ensuring optical and RF phase matching and an efficient electric field distribution across the electrodes. This approach guarantees the modulator's high-speed functionality with low power consumption.

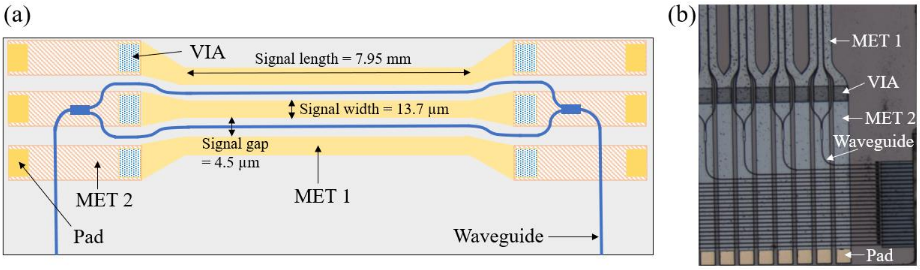

Fig. 1. (a) Schematic of the standard electro-optical modulator. (b) Optical image of the area of a fabricated TFLN with a series of EO modulators.

The devices are manufactured through a standard foundry process at CSEM on a 150 mm wafer scale. Our fabrication technique utilizes readily available thin-film lithium niobate on insulator (LNOI) wafers. These wafers consist of a layer of 600 nm thick mono-crystal x-cut LiNbO3 on top of a 4.7 µm buried thermal oxide (BOX) layer. This platform offers three different types of waveguides, providing designers with flexibility to create circuits optimized for various wavelengths. The PIC platform incorporates a dual-layer metallization structure that improves the routing process for radio frequencies, enabling more efficient signal transmission. All layers in the platform are shielded by a silicon oxide cladding. Additionally, a specialized layer known as "clad open" is included, giving designers the option to selectively remove the cladding. This feature allows for specific applications, such as creating access points to the metal pads or directly interfacing with the waveguides. The final chip release process results in smooth facets, a critical factor for achieving effective light coupling at both the input and output interfaces of the device. We have fabricated two identical modulators from two different wafers. In the following section we will compare their performances.

3 Experiment and Discussion

The complete performance evaluation of the modulator focuses on two principal domains: DC (Direct Current) for assessing modulation efficiency, and RF (Radio Frequency) measurements for investigating the overall modulator performances. The latter comprises Electrical-Electrical (EE) measurements, to evaluate the electrical losses and the design quality in terms of impedance matching and microwave-optical index matching, and Electro-Optical (EO) measurements, to evaluate the performance of the modulator at high frequency.

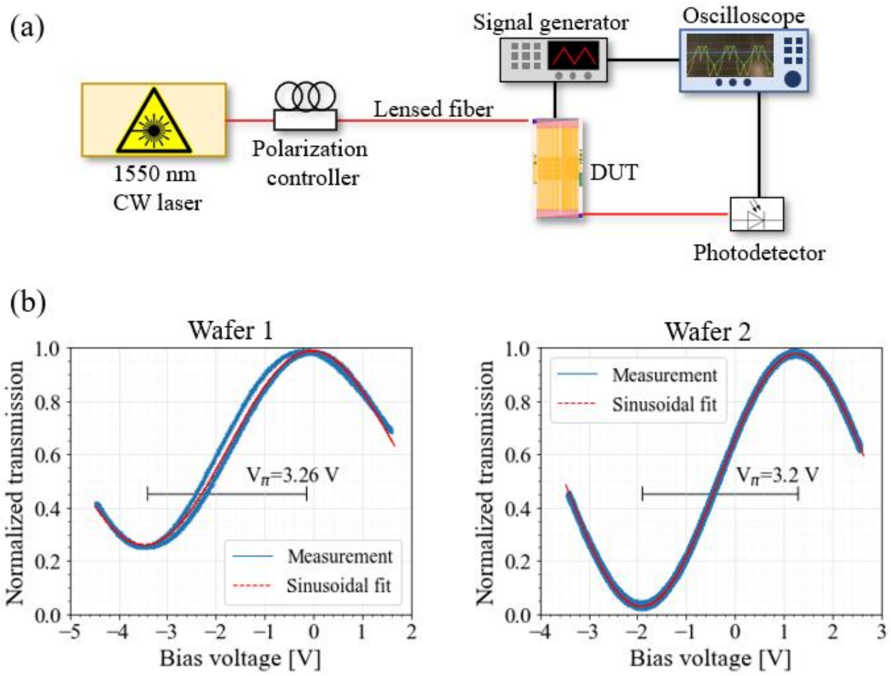

Fig. 2. Schematic of the experimental setups used for DC measurements (a) and DC electro-optical response of the modulators from wafer 1 and 2 (b).

Fig. 2(a) depicts the characterization setups used for DC measurements. To measure the half-wave voltage V_π of the modulator, a low frequency characterization has been performed; a triangular electrical signal with a frequency of 5 kHz was directly applied to the electrodes, and the modulated optical output was recorded by a photodetector, whose response was acquired using a 500 MHz bandwidth oscilloscope. Modulators from two different wafers show very similar performances, with a half-wave voltage of 3.26 V and 3.2 V in wafer 1 and 2, respectively (Fig. 2(b)). The devices show a voltage-length products of 2.59 V.cm and 2.54 V.cm in Wafer 1 and Wafer 2, respectively. The difference in ER between Wafer 1 and Wafer 2 could be attributed to a degraded beam splitters in the Wafer 1 due to fabrication defects. We also observe a hysteresis profile in Wafer 1 that is attributed to the DC drift of the modulator due to a non-optimized manufacturing steps parameters in Wafer 1.

Fig. 3(a) shows the setup used for RF measurements. Light from a mode hop-free laser emitting at 1550 nm was sent to the chip through a polarization controller and a lensed fiber. A DC bias was applied to drive the modulator at the quadrature point. A microwave signal was generated by a VNA (extending up to 50 GHz) and applied to the electrodes through ground-signal-ground electrical probes. The optical output was recorded by a fast photodetector and sent to the output port of the VNA. The relatively low electrical signal attenuation (Fig. 3(b)) allows to achieve high EE bandwidth (Fig. 3(d)), as the transmitted signal power decreases of about 6 dB at 50 GHz as compared to its value at the 1 GHz reference frequency. The microwave effective index extracted from measurements is around 2.85 at high frequency. This value is close to the optical group index of 2.28 retrieved from simulations (red line in Fig. 3(c)), yet an incomplete matching between the microwave and optical waves speed is a limiting factor for the modulator’s EO performances at high frequency. This aspect will be addressed in future design to further improve the performances of the device. A very low electrical signal reflection of below 20 dB (see Fig. 3(d)) indicates an excellent impedance matched circuitry. Fig. 3(e) shows the EO frequency response. The bandwidth exceeds 50 GHz, given that the output power hasn't decreased by 3 dB at this frequency (black dashed line in Fig. 3(e), calculated relatively to 1 GHz).

These findings highlight the device's significant potential to operate beyond 50 GHz bandwidth, a crucial milestone for required modulation schemes. Further refinements could focus on improving the metals quality to reduce the electrical losses, and to adjusting the modulator dimensions for a better microwave-optical index matching. These improvements could increase the bandwidth even further, potentially beyond 100 GHz, while pushing down the operation voltage towards CMOS levels.

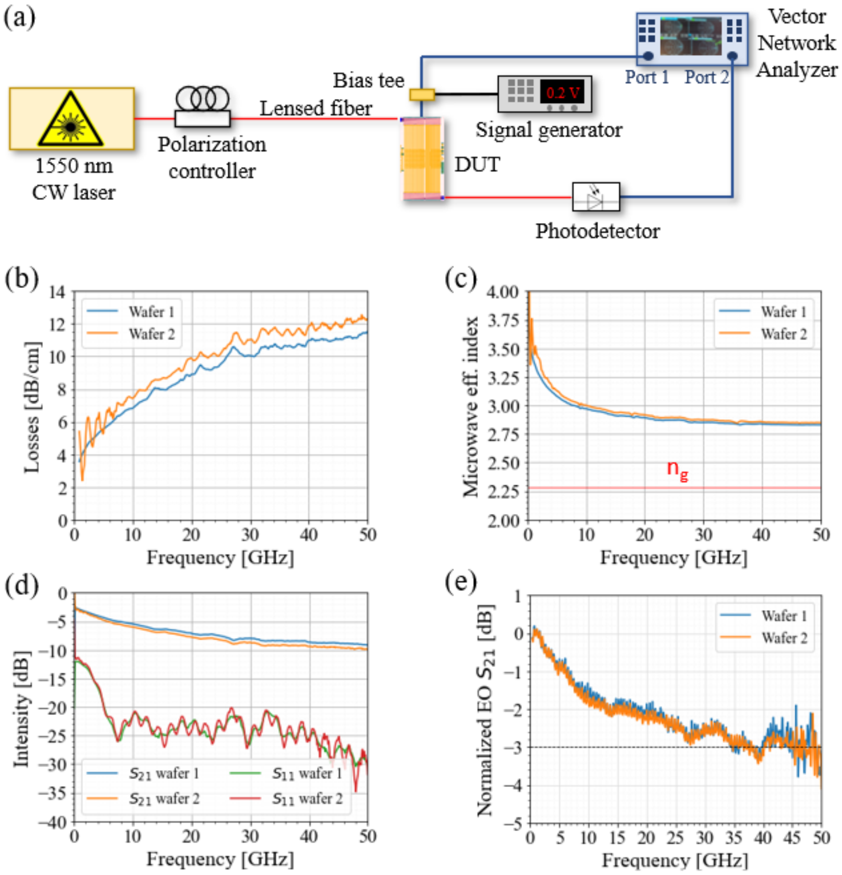

Fig. 3. **(a)** Schematic of the experimental setups used for DC measurements. (b) Measured electrical signal attenuation as a function of microwave frequency. (c) Measured microwave effective index (blue) and simulated optical group index (red). (d) Measured EE response. (e) Measured EO response normalized to 1 GHz.

4 Conclusion

We presented and compared a full characterization of two TFLN EO modulators, with an identical design but from two different wafers fabricated through our open-access foundry process. The modulators, operating in the telecom C-band show very similar performances, with an EO bandwidth surpassing 50 GHz and a half-wave voltage of around 3.2 V. This is an important starting point, evaluating the reliability of our foundry process, a crucial step towards the development of a standardized platform with a reliable PDK building blocks. Future work will focus on comparing the performances of modulators from a higher number of wafers, different locations on the wafer, and from different fabrication RUNs. According to the increasing demand for low power, high bandwidth photonic devices, developing of TFLN PICs in a standardized platform paves the way for fast, large-scale, and energy-efficient PIC systems, elusive via other PIC platforms.

Acknowledgments

This project has received funding from the European Union's Horizon 2020, GA No. 101016138; European Union Horizon under GA Nos. 101070506, 101070441 and 101070581.

References

1. Zhu, D. et al.: Integrated photonics on thin-film lithium niobate. Adv. Opt. Photon. 13(2), 242-352 (2021).
2. Liu, A. et al.: High-speed optical modulation based on carrier depletion in a silicon waveguide. Opt. Express 15(2), 660-668 (2007).
3. Harris, N. C. et al.: Efficient, compact and low loss thermo-optic phase shifter in silicon. Opt. Express 22(9), 10487-10493 (2014).
4. Errando-Herranz, C. et al.: MEMS for Photonic Integrated Circuits. IEEE Journal of Selected Topics in Quantum Electronics 26(2), 1-16 (2020).
5. Melikyan, A. et al.: High-speed Plasmonic Modulators. Nature Photonics 8, 229-233 (2014).
6. Zhang, M. et al.: Integrated lithium niobate electro-optic modulators: when performance meets scalability. Optica 8(5), 652-667 (2021).
7. Jin, M et al.: Efficient electro-optical modulation on thin-film lithium niobate. Opt. Letters 46, 1884-1887 (2021).
8. Weigel, P. O. et al.: Bonded thin film lithium niobate modulator on a silicon photonics platform exceeding 100 GHz 3-dB electrical modulation bandwidth. Opt. Express 26(18), 23728-23739 (2018).
9. Leo, J. et al.: Wafer-scale fabrication of low-loss waveguides in lithium niobate on insulator (LNOI) integrated photonics platform. In: European Conference on Optical Communication, Basel (2022).
10. Monney, A. et al.: Statistical characterization of MMI beam splitters on thin film lithium niobate on insulator (LNOI) platform at telecom wavelength. In: Conference on Lasers and Electro-Optics/Europe and European Quantum Electronics Conference, Munich (2023).